A theoretical and experimental NMR study of the prototropic tautomerism of tris(tetrabutylammonium) hydrogen pyrophosphate salt in solution and in the solid-state

Dionisia Sanz,[a] Rosa M. Claramunt,[a]* Ibon Alkorta,[b] José Elguero[b]
[a]Departamento de Química Orgánica y Bio-Orgánica, Facultad de Ciencias, UNED, Senda del Rey 9, 28040-Madrid, Spain
[b]Instituto de Química Médica, Centro de Química Orgánica Manuel Lora-Tamayo, CSIC, Juan de la Cierva 3, 28006-Madrid, Spain

Un estudio RMN teórico y experimental de la tautomería prototrópica del hidrógeno pirofosfato de tris(tetrabutilamonio) en solución y en estado sólido.

Estudi RMN teòric i experimental de la tautomeria prototròpica del hidrogen pirofosfat de tris(tetrabutilamoni) en solució i en l'estat sòlid

Recibido: 25 de mayo de 2014; aceptado: 14 de agosto de 2014

RESUMEN

La estructura del tris(tetrabutilamonio) hidrógeno pirofosfato (HPP) ha sido estudiada en disolución y en estado sólido por RMN de ^{31}P. Cálculos GIAO/DFT de la molécula aislada en sus conformaciones abierta y cerrada, de sus complejos con una molécula de agua y de los efectos de disolvente con un modelo del continuo han servido para discutir los datos experimentales de RMN. Contrariamente a los datos de la literatura, HPP da una señal única en disolución que se ensancha considerablemente al enfriar hasta 193 K sin alcanzar la coalescencia. En estado sólido se observan dos señales muy próximas que los cálculos no logran reproducir.

Palabras clave: Hidrógeno pirofosfato; solvatación; tautomería; ^{31}P RMN; CPMAS; GIAO.

SUMMARY

The structure of tris(tetrabutylammonium)hydrogen pyrophosphate (HPP) has been studied in solution and in the solid-state by ^{31}P NMR. GIAO/DFT calculations of the isolated molecule in its open and closed conformations, of their water complexes and the solvent effects (continuum model) have been useful to discuss the experimental NMR data. Contrary to literature reports, the ^{31}P NMR spectra of HPP in solution have a single band, that broadened considerably when the temperature is lowered till 193 K without reaching the coalescence. In the solid-state, two very close signals are observed that the calculations do not reproduce adequately.

Key words: Hydrogen pyrophosphate; solvation; tautomerism; ^{31}P RMN; CPMAS; GIAO.

RESUM

L'estructura del hidrogen pirofosfat (HPP) de tris(tetrabutilamoni) s'ha estudiat en solució i en l'estat sòlid per ^{31}P RMN. Càlculs GIAO/DFT de la molècula aïllada en les seves conformacions oberta i tancada, dels seus complexos amb una molècula d'aigua i dels efectes de dissolvent (model continu) han estat útils per discutir les dades experimentals de RMN. Contràriament a les dades de la literatura, HPP dóna un senyal única en solució que s'eixampla considerablement en refredar fins 193 K sense arribar a la coalescència. En estat sòlid s'observen dos senyals molt properes que els càlculs no reprodueixen adequadament.

Paraules clau: Hidrogen pirofosfat; solvatació, tautomeria; ^{31}P RMN; CPMAS; GIAO.

1. INTRODUCTION

Pyrophosphoric acid, $H_4P_2O_7$, and its salts (pyrophosphates) are important compounds in biology, biochemistry, medicine and food sciences. For instance tetrasodium pyrophosphate is often used as a food additive (1); chondrocalcinosis (calcium pyrophosphate dihydrate crystal deposition disease) is a rheumatological disorder due to accumulation of calcium pyrophosphate dihydrate in the connective tissues (2); but is its presence in ADP that constitutes its major interest (3). The anion $P_2O_7^{4-}$, PPi, is formed in cells by hydrolysis of ATP into AMP (4) while inositol pyrophosphates play a crucial role in diverse cellular processes (5,6).

Amongst the pyrophosphates, the tris(tetrabutylammonium) hydrogen pyrophosphate salt (TTBHPP) is commercially available (CAS Number 76947–02-9) and has been often used as a phosphorylating reagent (7,8,9,10,11,12).

In the field of anion recognition (13,14,15,16,17), TTBHPP being a salt of HPP ($HP_2O_7^{3-}$), is one of the frequently studied anions because it is soluble in organic solvents and because it bears three negative charges. Since it is a strong base, it can remove a proton from the host if it has acidic protons. It is known, for instance, that pyrrole could be deprotonated to pyrrolate anion by basic anions (18,19,20). Another characteristic of TTBHPP is its instability. It is sell with ≥ 97% purity (calculated on dry substance) which means that it contains water and about 3% of impurities, probably phosphorus derivatives. Since pyrophosphoric acid (PPA) reacts with water to yield phosphoric acid and that this, in turn, reacts with PPA to yield triphosphoric acid TPPA (or its salts), the major impurity could correspond to TPPA.

When, for determining the stability Ka constants by fluorescence (21,22) or by ^{1}H NMR using a proton of the host (23,24,25), there is no special problem with TTBHPP, on the other hand, if ^{31}P NMR is used (26,27,28,29), then it arises the question of how many ^{31}P NMR signals we should expect from HPP, one or two?

For instance, Ghosh et al. (28) reported the following results (Figure 1, the chemical shifts are from a personal communication from Prof. K. Ghosh) obtained in DMSO-d_6:

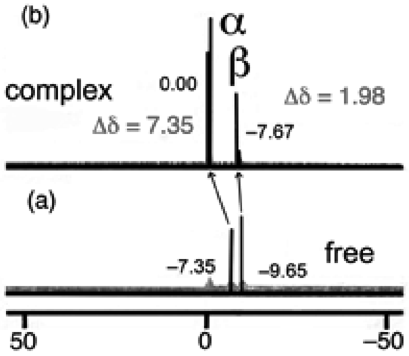

Figure 1. *Modified from reference 28*

Note that both ^{31}P atoms are separated by 2.3 ppm in the free HPP and also that in the complex one signal (assigned to the α ^{31}P) is considerable more intense than the other (assigned to the β ^{31}P).

There is a formal analogy between hydrogen pyrophosphate trianion (HPP) and the enol of acetylacetone (Figure 2):

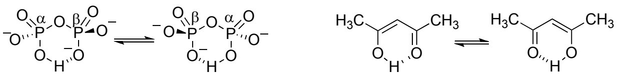

Figure 2. *Intramolecular proton transfers between identical tautomers.*

The intramolecular proton transfer should be very fast in both cases. In the enol, only in the solid-state and inside of a host cavity both tautomers appear different (30). Thus, we decided to examine the case of HPP suspecting that when two ^{31}P NMR signals were observed in solution, one (the most intense) belongs to HPP and the other (the less intense) to an impurity.

2. COMPUTATIONAL DETAILS

Calculations were carried out at the B3LYP/6-311++G(d,p) level using the facilities of the Gaussian 09 series of programs (31,32,33,34,35). The structures were characterized as minima or transition states by mean of their imaginary frequencies, either 0 or 1. Solvent effects were calculated using the PCM method (36). ^{31}P absolute shieldings were calculated within the GIAO approximation (37,38) and transformed into chemical shifts by means of the following equation (39):

$$^{31}\text{P exp.} = 222.8 - 0.75\ ^{31}\text{P calcd.} \qquad \text{Eq. 1.}$$

3. NMR EXPERIMENTS

Solution ^{31}P NMR spectra were recorded on a Bruker DRX 400 (9.4 Tesla, 161.96 MHz for ^{31}P) spectrometer with a 5-mm inverse-detection H-X probe equipped with a Bruker BVT3000 temperature unit to control the temperature of the cooling gas stream and an exchanger to achieve low temperatures. To avoid problems at low temperatures caused by air moisture, pure nitrogen was used as bearing, driving and cooling gas.

The chemical shifts (δ in ppm) are reported from external standard, a 85% w/w H_3PO_4 solution (δ = 0 ppm).

Solid-state ^{31}P CPMAS NMR spectra have been obtained on a Bruker WB 400 spectrometer (162.16 MHz for ^{31}P) at 300 K using a 4 mm DVT probehead. Samples were carefully packed in a 4-mm diameter cylindrical zirconia rotor with Kel-F end-caps. ^{31}P spectra were referenced to $(NH_4)_2HPO_4$ (AHP). Typical acquisition parameters for ^{31}P CPMAS were: spectral width, 100 kHz; recycle delay, 60 s; acquisition time, 40 ms; contact time, 2 ms; and spin rate, 10 and 12 kHz.

Single-pulse spectra were acquired on a Bruker Avance III 600 WB spectrometer with a magnetic field of 14.09 T and equipped with a MAS NMR multinuclear probe. Powdered samples were packed in 4 mm zirconia rotors and spun at 15 KHz. ^{31}P MAS-NMR spectra were acquired at a frequency of 242.94 MHz, using a single pulse program with a π/2 pulse width of 4.8 μs and a pulse space of 200 s and the number of scans were 62, 128 and 256.

4. RESULTS AND DISCUSSION

Theoretical results.

There are two possible structures for HPP, one presenting an intramolecular hydrogen bond (IMHB, Cs symmetry, Figure left 3,“closed”) and the other with the OH pointing outside the molecule (Figure right 3,“open”). The first is the most stable in the gas phase and the second one in DMSO

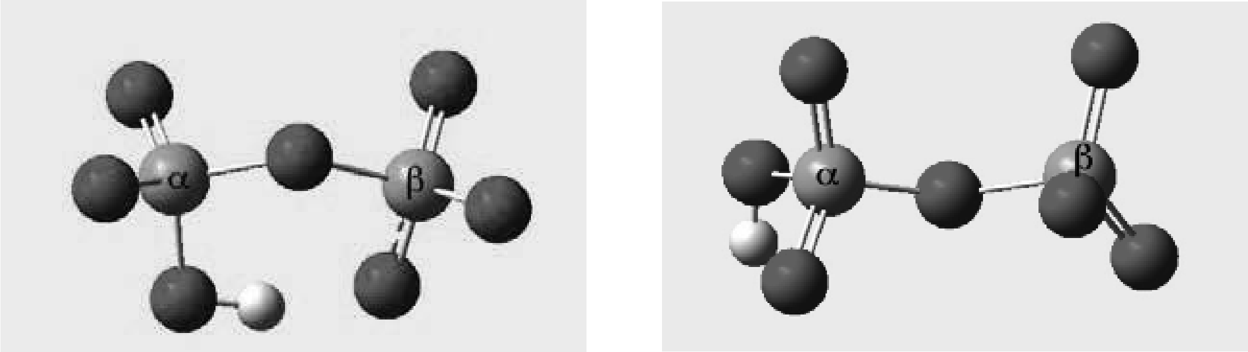

Figure 3. *Minimum energy geometries of HPP.*

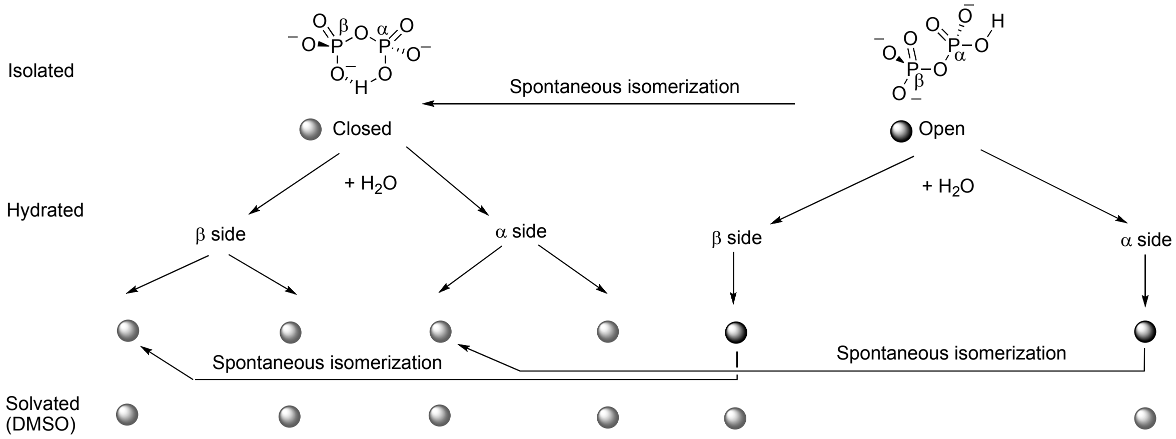

Figure 4. *In red all the localized minima; in grey, structures that isomerize into red ones.*

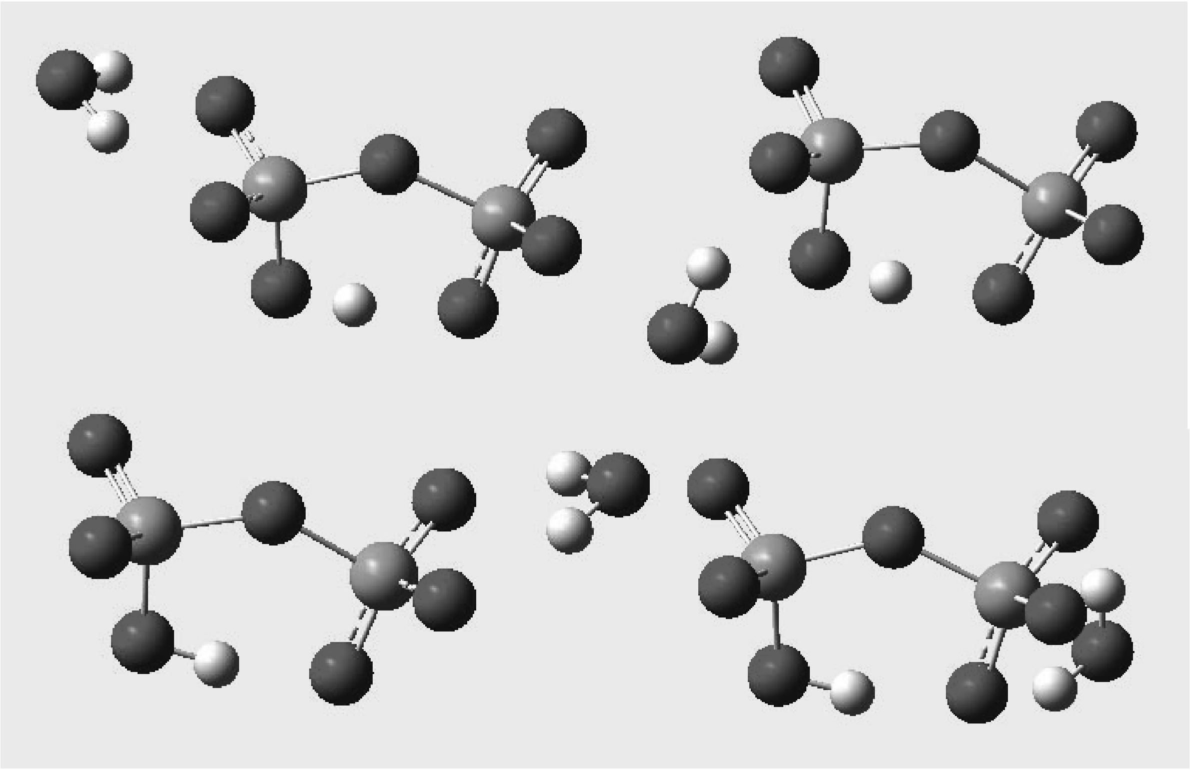

Figure 5. *The four hydrated minima of the closed isomer: top α side; bottom β side.*

In the gas-phase, the TS corresponding to the intramolecular proton transfer of the IMHB form with C_{2v} symmetry (see Figures 2 and 3) has a value of 7.9 that decreases to –1.6 kJ·mol^{-1} when the ZPE is included (i.e. the TS is more stable than the minima), in any case, corresponds to a low-barrier hydrogen-bond (LBHB) (40).

Besides the calculation of the isolated monomers in the gas-phase where only the HB structure “closed” is stable, we have carried out a series of calculations that we have summarized in Figure 4.

Table 1. *Calculated ^{31}P chemical shifts of HPP.*

Compound	Phase	α (P6)	β (P1)	Difference	Mean
HB	gas*	+2.69	+16.38	13.69	9.54
	acetone	+0.17	+9.72	9.55	4.94
	CH_3CN	+0.14	+9.56	9.42	4.85
	DMSO	+0.20	+9.57	9.37	4.88
HB + H_2O α side, position 1	gas	–0.09	+16.30	16.39	8.10
	DMSO	–2.02	+9.76	11.78	3.87
HB + H_2O α side, position 2	gas	+2.85	+16.70	13.85	9.78
	DMSO	+0.22	+9.60	9.38	4.91
HB + H_2O β side, position 1	gas	+0.95	+11.71	10.76	6.33
	DMSO	+0.02	+7.66	7.64	3.84
HB + H_2O β side, position 2	gas	+0.69	+10.53	9.84	5.61
	DMSO	–0.88	6.50	7.38	2.81
OH outside	gas**	----	----	----	----
	acetone	–1.87	+13.74	15.61	5.94
	CH_3CN	–1.89	+13.52	15.41	5.82
	DMSO	–1.88	+13.47	15.35	5.80
OH outside + H2O α side	DMSO	–2.88	+14.19	17.07	5.66
OH outside + H2O β side	DMSO	–3.05	+8.68	11.73	2.82

* Calculated $^2J_{PP}$ = –45 Hz.

** This “open” structure isomerizes during the optimization to the HB “closed” isomer.

On the isolated monomers we have calculated solvent effects using the PCM approximation (acetone, CH_3CN and DMSO). Then, we have solvated by a water molecule each isomer on both sides, the hydrated open structures isomerize into the closed isomers but, when solvated by DMSO, they are stable. For the closed isomer, that has a symmetry plane, there are two kinds of oxygen atoms and both minima have been located (Figure 5). In all, ten hydrated minima have been found and the corresponding ^{31}P chemical shifts calculated. They are reported in Table 1.

The absolute values are not very reliable because Eq. 1 has a low correlation coefficient (R^2 = 0.847, twenty points) and because a trianion is rather different from the molecules that were used to establish such equation. On the other hand, the differences should be more reliable.

^{31}P NMR solution studies.

We have carried out a series of experiments in a 400 MHz instrument working at 9.4 T, i.e. 162 MHz for ^{31}P using different solvents and different temperatures. **In all cases only one signal was observed for HPP** (Figure 6). Besides, an AB_2 system (a triplet corresponding to the central ^{31}P and a doublet corresponding to both external ^{31}P atoms with $^3J_{PP}$ = 28 Hz, probably –28 Hz according to the calculations of Table 1) of small intensity was observed that corresponds most probably to a hydrogen triphosphate anion (number of protons and negative charges undetermined). This indicates that, if there is proton transfer in the hydrogen triphosphate, it is very fast because the signals are narrow.

In Figure 6a the singlet (slightly broad) of HPP and the AB_2 system of triphosphate in DMSO-d_6 are shown. The broadening of the HPP signal is solvent dependent (Δ is the full width at half maximum in Hz) as reported in Figure 6b. The broadening also increases when the temperature is lowered (Figure 6c in acetone-d_6 and Figure 6d in THF-d_8). These data indicate that the proton transfer is slowed down by dipolar aprotic solvents such as DMSO and HMPA as well as by lowering the temperature although at 193 K in acetone the signal is still not very broad. In THF at 213 K the broadening is considerable but the coalescence temperature was not reached. The signal at –8.6 ppm (smaller in intensity) belongs to an impurity.

Assuming that the coalescence temperature in acetone is Tc = 190 K and that the separation of the signals is Δν = 7.4 ppm = 1895 Hz (see Table 1, HB + H_2O β side, position 2 in DMSO), the Eyring equation affords a barrier of ~31 kJ·mol^{-1}. For Δν = 0.53 ppm = 86 Hz (see below, solid-state), the Eyring equation affords a barrier of ~39 kJ·mol^{-1}. Although these barriers are rough estimates it is clear that they are incompatible with the HB structure with its almost null barrier. We conclude then that HPP in solution exists as the “open” structure.

Amongst the OH outside forms, the closest calculated value to the –3.9 ppm chemical shift measured in DMSO-d_6 is that corresponding to the complex with a water molecule on the β side (2.82 ppm) with a Δν = 11.7 ppm (vide supra). Thus, Eq. 1 predictions for HPP have an error of 6-7 ppm, but bear in mind that ^{31}P NMR chemical shifts cover a range of ~1500 ppm (41).

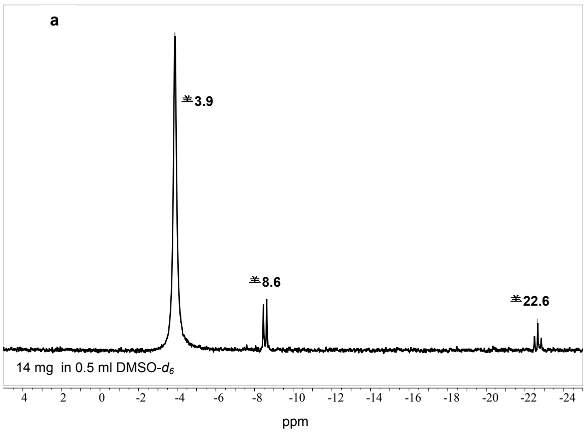

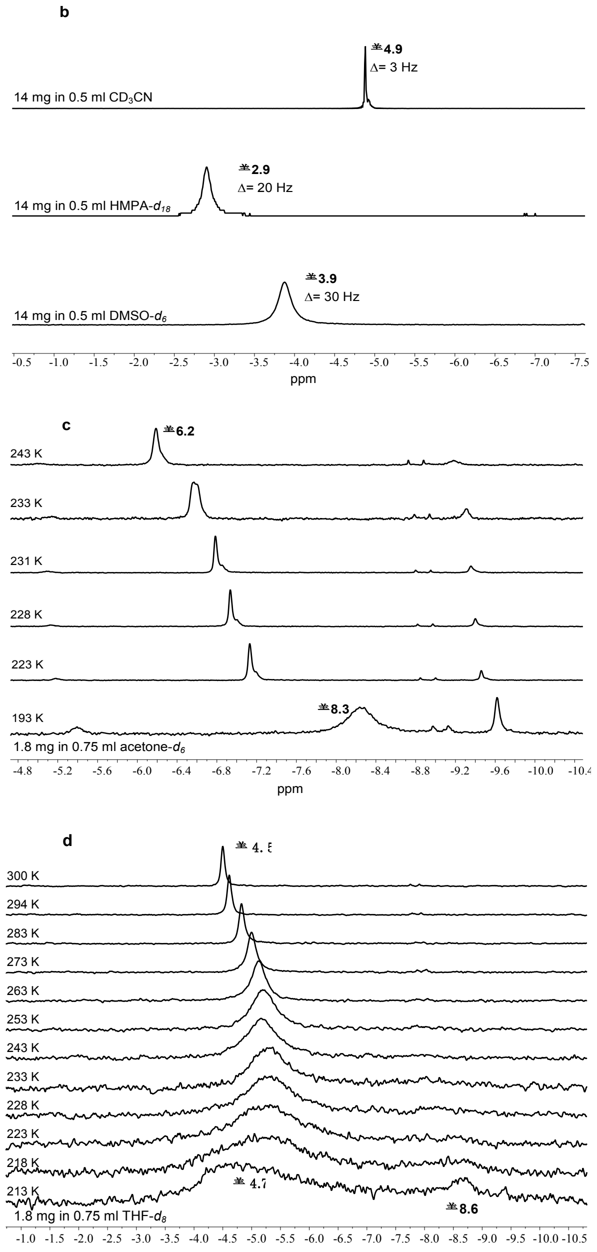

Figure 6. *Some ^{31}P NMR spectra of HPP in solution.*

^{31}P NMR solid-state studies.

We have recorded the ^{31}P MAS spectrum of HPP in many different conditions both at 9.4 (162 MHz) and 14.1 T (243 MHz) obtaining different spectra with one or two signals of different intensities and with the smaller signal to the right and to the left of the larger one. The increase of the field does not improve the resolution. In Figure 7 it is represented the nicer spectrum we have recorded (9.4 T, rotating rate 10,000 Hz, ^{1}H high power decoupling, 4 mm DVT probehead). The mean chemical shift (–4.1 ppm) is close to that measured in DMSO-d_6.

The spectrum seems to correspond to an AB system. The separation of the signals is very small (0.53 ppm, $\Delta\nu_{AB}$ = 86 Hz) and the J_{AB} = $^2J_{PP}$ = 31.8 Hz has a reasonable value (see Figure 6a) for HPP. Figure 7 could correspond to a structure solvated by water since the compound is sold non-dryed. However, the intensities are different and this indicates that the spectrum of Figure 7 must be considered only a preliminary result. Unfortunately, a series of experiments carried out at 9.4 and 14.1 T (Figure 8) shows that the appearance of the spectra is very sensitive to the recording conditions.

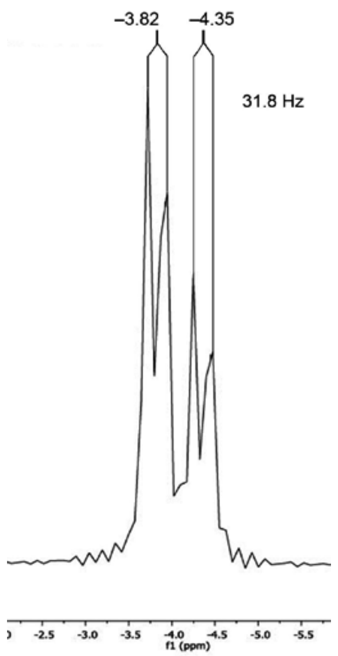

Figure 7. *^{31}P MAS spectrum of HPP.*

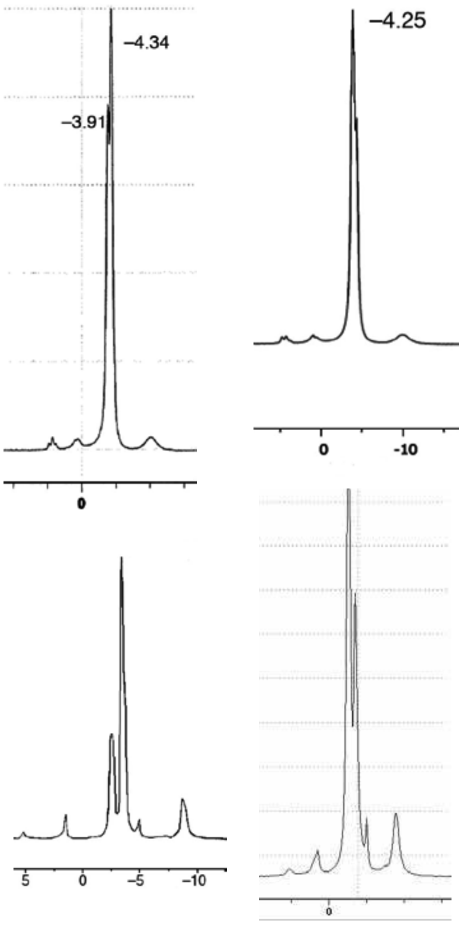

Figure 8. *^{31}P MAS spectra of HPP: top at 9.4 T; bottom at 14.1 T.*

5. CONCLUSIONS

There is no X-ray structure available for tris(tetrabutylammonium)hydrogen pyrophosphate, but the present solid-state ^{31}P NMR results are indicative of a IMHB structure. Recently, Nishida et al. (42) reported the study of SnHPP doped with Mg, In and Al finding only broad singlets. If our solid-state results deserve further investigation, our solution studies clearly conclude that at room temperature, HPP appears in ^{31}P NMR as a unique signal.

ACKNOWLEDGEMENTS

This work was financed by the Ministerio de Economía y Competitividad of Spain (Projects CTQ20010-16122 and CTQ2012-35513-C02-02) and the Comunidad Autónoma de Madrid (Project MADRISOLAR2, ref. S2009/PPQ-1533). Professor H.-H. Limbach comments are greatly acknowledged.

REFERENCES

1. List of Codex specifications for food additives (CAC/MISC 6-2013).
2. M. Doherty, New insights into the epidemiology of gout, Rheumatology 48, ii2–ii8 (2009).
3. D.R. Ferrier, R.A. Harvey, P.M. Champe, Biochemistry, Six Edition, Lippincott Williams & Wilkins, Philadelphia, 2014.
4. Nucleic Acids from A to Z, Ed. S. Müller, Wiley-VCH, Weinheim, 2008.
5. C.J. Barker, C. Illies, G.C. Gaboardi, P.O. Berggren, Inositol pyrophosphates: structure, enzymology and function, Cell. Mol. Life Sci. 66, 3851–3871 (2009).
6. J. Worley, X. Luo, A.P. Capaldi, Inositol pyrophosphates regulate cell growth and the environmental stress response by activating the HDAC Rpd3L, Cell Reports 3, 1476–1482 (2013).
7. V.M. Dixit, F.M. Laskovics, W.I. Noall, C.D. Poulter, Tris(tetra-n-butylammonium) hydrogen pyrophosphate. A new reagent for the preparation of allylic pyrophosphate esters, J. Org. Chem. 46, 1967–1969 (1981).
8. V.J. Davisson, D.R. Davis, V.M. Dixit, C.D. Poulter, Synthesis of nucleotide 5’-diphosphates from 5’-O-tosyl nucleosides, J. Org. Chem. 52, 1794–1801 (1987).
9. A.B. Woodside, Z. Huang, C.D. Poulter, Trisammonium geranyl diphosphate, Org. Synth. 66, 211–219 (1988).
10. F. Seela, H.P. Muth, A. Röling, Syntheses of Pyrrolo[2,3-d]pyrimidine 2’,3’-Dideoxyribonucleosides Related to 2’,3’-Dideoxyadenosine and 2’,3’-Dideoxyguanosine and Inhibitory Activity of 5’-Triphosphates on HIV-1 Reverse Transcriptase, Helv. Chim. Acta 74, 554–564 (1991).
11. D. Sun, H. Xu, S.R. Wijerathna, C. Dealwis, R.E. Lee, Structure-based design, synthesis, and evaluation of 2’-(2-hydroxyethyl)-2’-deoxyadenosine and the 5’-diphosphate derivative as ribonucleotide reductase inhibitors, ChemMedChem 4, 1649–1656 (2009).
12. T. Santner, V. Siegmund, A. Marx, R. Micura, The synthesis of 2’-metjylseleno adenosine and guanosine 5’-triphosphates, Bioorg. Med. Chem. 20, 2416–2418 (2012).
13. Supramolecular Chemistry of Anions, Eds. A. Bianchi, K. Bowman-James, E. García-España, Wiley-VCH, New York, 1997.
14. J.L. Sessler, P. Gale, W.S. Cho, Anion Receptor Chemistry, Ed. J.F. Stoddart, RSC Publishing, Cambridge, U.K., 2006.
15. Recognition of Anions, Ed. R. Vilar, Struct. Bond. Springer-Verlag, Berlin, Vol. 129, 2008.
16. Anion Recognition in Supramolecular Chemistry, Eds. P.A. Gale, W. Dehaen, Top. Heterocycl. Chem., Springer-Verlag, Berlin, Vol. 24, 2010.
17. Anion Coordination Chemistry, Eds. K. Bowman-James, A. Bianchi, E. García-España, Wiley-VCH, Weinheim, 2011.
18. S. Camiolo, P.A. Gale, M.B. Hurtshouse, M.E. Light, A.J. Shi, Solution and solid-state studies of 3,4-dichloro-2,5-diamidopyrroles: formation of an unusual anionic narcissistic dimer, Chem. Commun. 758–759 (2002).
19. S. Camiolo, P.A. Gale, M.B. Hurtshouse, M.E. Light, Nitrophenyl derivatives of pyrrole 2,5-diamides: structural behaviour, anion binding and colour change signalled deprotonation, Org. Biomol. Chem. 1, 741–744 (2003).
20. P.A. Gale, Structural and molecular recognition studies with acyclic anion receptors, Acc. Chem. Res. 39, 465–475 (2006).
21. T. Gunnlaugsson, A.P. Davis, J.E. O’Brien, M. Glynn, Fluorescent sensing of pyrophosphate and bis-carboxylates with charge neutral PET chemosensors, Org. Lett. 4, 2449–2452 (2002).
22. R. Martínez-Mañez, F. Sancenón, New advances in fluorogenic anion chemosensors, J. Fluoresc. 15, 267–285 (2005).
23. J.Y. Kwon, Y.J. Jang, S.K. Kim, K.H. Lee, J.S. Kim, J. Yoon, Unique hydrogen bonds between 9-anthracenyl hydrogen and anions, J. Org. Chem. 69, 5155–5157 (2004).
24. S.K. Kim, N.J. Singh, J. Kwo, I.C. Hwang, S.J. Park, K.S. Kim, J. Yoon, Fluorescent imidazolium receptors for recognition of pyrophosphate, Tetrahedron 62, 6065–6072 (2006).
25. J.L. Sessler, J. Cai, H.Y. Gong, X. Yang, J.F. Arambula, B.P. Hay, A pyrrolyl-based triazolophane: A macrocyclic receptor with CH and NH donor groups that exhibits a preference for pyrophosphate anions, J. Am. Chem. Soc. 132, 14058–14060 (2010).
26. A.E. Hargrove, S. Nieto, T. Zhang, J.L. Sessler, E.V. Anslyn, Artificial receptors for the recognition of phosphorylated molecules, Chem. Rev. 111, 6603–6782 (2011).
27. F. Zapata, A. Caballero, A. Espinosa, A. Tárraga, P. Molina, Cation coordination induced modulation of the anion sensing properties of a ferrocene-imidazophenantholine dyad: multichannel recognition from phosphate-related to chloride anions, J. Org. Chem. 73, 4034–4044 (2008).
28. K. Ghosh, A.R. Sarkar, A. Samadder, A.R. Khuda-Bukhsh, Pyridinium-based fluororeceptors as practical chemosensors for hydrogen pyrophosphate

($HP_2O_7^{3-}$) on semiaqueous and aqueous environments, Org. Lett. 14, 4314–4317 (2012).

29. A. Caballero, F. Zapata, L. González, P. Molina, I. Alkorta, J. Elguero, Discovery of anion-π interactions in the recognition mechanism of inorganic anions by 1,2,3-triazolium rings, Chem. Commun. 50, 4680–4682 (2014).
30. R.M. Claramunt, C.López, S. Lott, M.D. Santa María, I. Alkorta, J. Elguero, Solid-state NMR study of the tautomerism of acetylacetone included in a host matrix, Helv. Chim. Acta 88, 1931–1942 (2005).
31. C. Lee, W. Yang, R.G. Parr, Development of the Colle-Salvetti correlation-energy formula into a functional of the electron density. Phys. Rev. B 37, 785–789 (1988).
32. A.D. Becke, Density-functional exchange-energy approximation with correct asymptotic behavior. Phys. Rev. A 38, 3098–3100 (1988)
33. R. Ditchfield, W.J. Hehre, J.A. Pople, Self-Consistent Molecular Orbital Methods. IX. An Extended Gaussian-Type Basis for Molecular Orbital Studies of Organic Molecules. J. Chem. Phys. 54, 724-728 (1971).
34. M.J. Frisch, J.A. Pople, J.S. Binkley, Self-Consistent Molecular Orbital Methods 25. Supplementary Functions for Gaussian Basis Sets. J. Chem. Phys. 80, 3265-3269 (1980).
35. Gaussian 09, Revision A.1, M.J. Frisch, G.W. Trucks, H.B. Schlegel, G.E. Scuseria, M.A. Robb, J.R. Cheeseman, G. Scalmani, V. Barone, B. Mennucci, G.A. Petersson, H. Nakatsuji, M. Caricato, X. Li, H.P. Hratchian, A.F. Izmaylov, J. Bloino, G. Zheng, J.L. Sonnenberg, M. Hada, M. Ehara, K. Toyota, R. Fukuda, J. Hasegawa, M. Ishida, T. Nakajima, Y. Honda, O. Kitao, H. Nakai, T. Vreven, J.A. Montgomery, Jr., J.E. Peralta, F. Ogliaro, M. Bearpark, J.J. Heyd, E. Brothers, K.N. Kudin, V.N. Staroverov, R. Kobayashi, J. Normand, K. Raghavachari, A. Rendell, J.C. Burant, S.S. Iyengar, J. Tomasi, M. Cossi, N. Rega, J. M. Millam, M. Klene, J.E. Knox, J.B. Cross, V. Bakken, C. Adamo, J. Jaramillo, R. Gomperts, R.E. Stratmann, O. Yazyev, A.J. Austin, R. Cammi, C. Pomelli, J.W. Ochterski, R.L. Martin, K. Morokuma, V.G. Zakrzewski, G.A. Voth, P. Salvador, J.J. Dannenberg, S. Dapprich, A.D. Daniels, Ö. Farkas, J.B. Foresman, J.V. Ortiz, J. Cioslowski, D.J. Fox, Gaussian, Inc., Wallingford CT, 2009.
36. B. Mennucci, R. Cammi, Eds. Continuum Solvation Models in Chemical Physics. From Theory to Applications. Chichester, John Wiley & Sons, 2007.
37. F. London, Quantum theory of interatomic currents in aromatic compounds, J. Phys. Radium 8, 397–409 (1937).
38. R. Ditchfield, Self-consistent Perturbation Theory of Diamagnetism. I. A Gauge-Invariant LCAO (Linear Combination of Atomic Orbitals) Method for NMR Chemical Shifts, Mol. Phys. 27, 789-807 (1974).
39. I. Alkorta, F. Blanco, J. Elguero, J. Mol. Struct. Theochem 42, 1–6 (2010).
40. W.W. Cleland, M.M. Kreevoy, Low-barrier hydrogen bonds and enzymic catalysis. Science 264, 1887–1890 (1994).
41. S. Berger, S. Braun, H.O. Kalinowski, NMR Spectroscopy of the Non-Metallic Elements, John Wiely & Sons, New York, 1997.
42. M. Nishida, T. Tanaka, H. Fukaya, W. Kanematsu, Solid-state NMR study of dopant effects on the chemical properties of Mg-, In-, and Al-doped SnP_2O_7, Magn. Reson. Chem. 52, 163–171 (2014).